



ISSN: 0067-2904

Effect of the Pulsed Laser Energy on the Properties of CdO: NiO Composite Thin Films for Solar Cell Applications

Khamees D. Mahmood ^{1*}, Kadhim A. Aadim ², Mohammed G. Hamed ¹

¹Department of Physics, College of Science, University of Anbar, Anbar, Iraq

² Department of Physics, College of Science, University of Baghdad, Baghdad, Iraq

Received: 4/4/2021

Accepted: 3/6/2021

Abstract

In this work, thin films of cadmium oxide: nickel oxide (CdO: NiO) were prepared by pulsed laser deposition at different pulse energies of Nd: YAG laser. The thin films' properties were determined by various techniques to study the effect of pulse laser energy on thin films' properties. X-ray diffraction measurements showed a mixture of both phases. The degree of crystallinity and the lattice constant increase with the laser energy increase, while the lattice strain decreases. FE-SEM images show that the substrates' entire surface is uniformly covered, without any cracks, with a well-connected structure consisting of small spherical particles ranging in size from 15 to 120 nm. Increasing the laser power causes to increase the particle size irregularly. EDX analysis showed increased oxidation in the samples using laser energy. The AFM of the thin film deposited at minimum energy shows the uniform deposition of samples prepared at the lowest energy. They are increasing pulses energy of the laser cause to increase in the average particle diameter and surface roughness. The charge carrier concentration decreases, and its mobility increases with laser energy. The I-V characteristics for CdO: NiO/porous-PSi heterojunctions prepared by different laser energies show photovoltaic properties. Optimum efficiency of the samples prepared with the lowest laser energy.

Keywords: pulsed laser deposition, CdO: NiO composite, Structural, Optical.

أغشية مزيج أكسيد الكاديوم: أكسيد النيكل الرقيقة تأثير طاقة الليزر النبضية على خصائص لتطبيقات الخلايا الشمسية

خميس ضاري محمود^{1*}، كاظم عبد الواحد عادم²، محمد غازي حمد¹

¹قسم الفيزياء، كلية العلوم، جامعة الانبار، الانبار، العراق

²قسم الفيزياء، كلية العلوم، جامعة بغداد، بغداد، العراق

الخلاصة

في هذا العمل ، تم تحضير أغشية رقيقة من أكسيد الكاديوم: أكسيد النيكل (CdO: NiO) عن طريق الترسيب الليزر النبضي عند طاقات نبضة مختلفة من ليزر النيودينيوم-ياك. تم تحديد خصائص الأغشية الرقيقة بتقنيات مختلفة لدراسة تأثير طاقة الليزر على خواص الأغشية الرقيقة المحضرة. أظهرت قياسات حيود

* Email: khameesdhari@gmail.com

الأشعة السينية مزيجًا من طورين. تزداد درجة التبلور وكذلك ثابت الشبكة مع زيادة طاقة الليزر، بينما يقل إجهاد الشبكة. تُظهر صور FE-SEM أن السطح الكامل للركائز مغطى بشكل موحد، دون أي تشققات، بهيكل متصل جيدًا يتكون من جزيئات كروية صغيرة يتراوح حجمها من 15 إلى 120 نانومتر. أدت زيادة طاقة نبضات الليزر إلى زيادة حجم الجسيمات بشكل غير منتظم. أظهر تحليل EDX زيادة الأكسدة في العينات باستخدام طاقة ليزر أعلى. تظهر قياسات AFM للأغشية الرقيقة المرسب عند الطاقة الدنيا ترسيب منتظم للعينات المحضرة. تؤدي زيادة الليزر إلى زيادة متوسط قطر الجسيمات وخشونة السطح. ينخفض تركيز حامل الشحنة وتزداد تحركيتها مع طاقة الليزر. تظهر خصائص التيار-فولتية للمفروق المتباين لأوكسيد الكادميوم: أوكسيد النيكل / السليكون المسامي المحضر بطاقات ليزر مختلفة خصائص كهروضوئية. الكفاءة المثلى للعينات المحضرة كانت بأقل طاقة ليزر.

1. Introduction

Environmentally stable solar cells are essential to meet future renewable energy demands. Therefore, it is necessary to choose materials such as metal oxides which are considered low-cost materials [1]. Cadmium Oxide (CdO) is one of these materials with good specifications controlled according to deposition parameters [2]. In general, CdO is an n-type metal oxide due to a lack of oxidization that causes oxygen vacancies within its lattice [3]. It can be used as a transparent conductive layer [4] or as a window layer in solar cells applications and other optoelectronic devices [5]. CdO thin films' properties, such as surface morphology, energy gap, concentration of charge carriers and mobility have been improved or changed by making composites with many other materials such as semiconductors [6]. Synthesis technique and parameters affect its properties. There are different techniques, such as thermal evaporation [7], sputtering [8], spray pyrolysis [9], pulsed laser deposition [10] etc., to deposit pure or mixed with other substances CdO thin film. Transformation of the material into a nanoscale leads to a change in its properties and a change in the nanoparticle's size or shape leads to a fundamental change in these thin films' properties. One of the most fundamental changes that occur to nanomaterials is the increase in the effective surface area, which leads to an increase in the atoms that interact directly with the environment and which are included in many applications such as gas sensors [11]. The other fundamental property is the phenomenon of quantum confinement, which has two significant effects. The first is increasing the semiconductor band gap, and the second is creating energy levels near the valence and conducting bands edges [12].

Nickel (III) oxide exhibits many unique optical, magnetic, electrical and chemical properties. It has great potential in applications such as in ceramic materials, electronic components, sensors, magnetic data storage materials and catalysts [13]. It was observed that nickel doping of CdO is efficient in obtaining high mobility in comparison to other dopants and could be used in optoelectronic applications [14].

In this work, the effect of the energy of pulsed laser on the properties (structural, surface morphology, optical, and electrical properties) of CdO: NiO composite thin film was investigated. In addition the current-voltage characteristic curves for the CdO: NiO/Porous-Si heterojunction were studied.

2. Experimental

Cadmium oxide (CdO) and nickel oxide (NiO) powders with 99.9% purity (from Sigma Aldrich), were mixed together by ball milling as powder mixer as 1:1 molar ratio and pressed as a pellet of 2 g weight and 1.5 cm diameter into a stainless-steel mould with a hydraulic piston under 8 tons pressure for 10 minutes. CdO: NiO composite thin films were deposited on glass substrates, which were previously cleaned, by pulsed laser deposition in a vacuumed chamber at 10^{-2} mbar using a dual-stage rotary pump. Laser beam was focused onto a spot on the target surface (of 1 mm diameter) by a 10 cm focal length lens with 45 degree. The deposition was done using Nd-Yag pulsed laser (DIAMOND-288) of fundamental

wavelength 1064 nm of 10 ns pulse duration at different pulse energies (300, 400, 500 and, 600 mJ) using 300 pulses. The substrate was positioned at 3 cm above the target surface. The physical properties and structural properties of the thin films were characterized with X-ray diffractometer (Shimadzu XRD 6000), atomic force microscope (mode AA3000 Scanning Probe Angstrom Advance Inc.), and by Hall effect measurements (Ecopia HMS-3000). Thickness of the thin films was measured with a reflectance probe (SR300 Angstrom Sun Technologies). Thin films thicknesses were 180, 210, 235, and 258 nm corresponding to the samples prepared by laser energy of 300, 400, 500 and, 600 mJ, respectively. Porous silicon structure (P-Si) was prepared by electrochemical etching of P-type silicon wafer, of (100) orientation and resistivity of 0.01 Ω .cm, in Teflon cell by two-electrode configuration with a platinum counter electrode and a silicon wafer anode. Etching time was 10 min with a current of 10 mA. Diluted hydrofluoric acid (HF) at (1:10) ratio with diode laser source aid as an illumination source. The result P-Si on silicon wafer is shown in Figure 1.

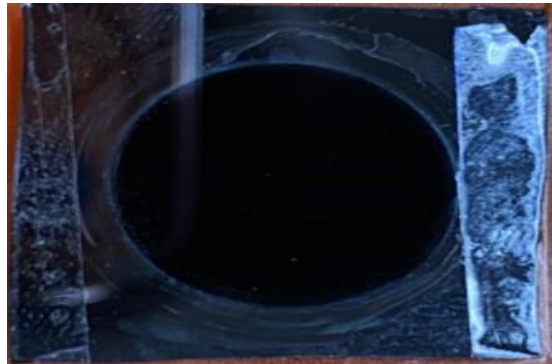


Figure 1- P-Si layers prepared on Si wafer.

The CdO: NiO composite thin films were prepared on the P-Si by different laser energies. The I-V characteristic curves of heterojunctions were examined to study the effect of laser energy used in sample preparation on heterojunction characteristics.

3. Results and discussions

Figure 2 shows the X-ray diffraction patterns for CdO: NiO composite thin films, prepared using different laser energies, compared with the standard cards of CdO and NiO. All samples showed polycrystalline structure of a significant mixed phase of CdO. The minor phase of NiO structure identical to the standard cards (96-900-8610 and 96-432-0488) cubic-CdO and cubic-NiO, respectively. It seems that cadmium oxide tends to crystallize with a greater degree than nickel oxide because it requires less energy to crystallize [15]. Increasing the laser energy caused enhancement of crystallinity, especially for the CdO phase. Table 1 lists the X-ray diffraction parameters for CdO: NiO thin films prepared by different laser energies. The variations in peaks location with increasing laser energy indicate variation in lattice strain [16]. The crystallinity enhanced by laser energy is due to increasing the ablated material and the merging of the adjacent small particles by removing the grain boundaries [17]. It is noted from the figure that cadmium oxide content dominates the thin film samples compared to nickel oxide due to the difference between the two mixed materials in the evaporation temperature.

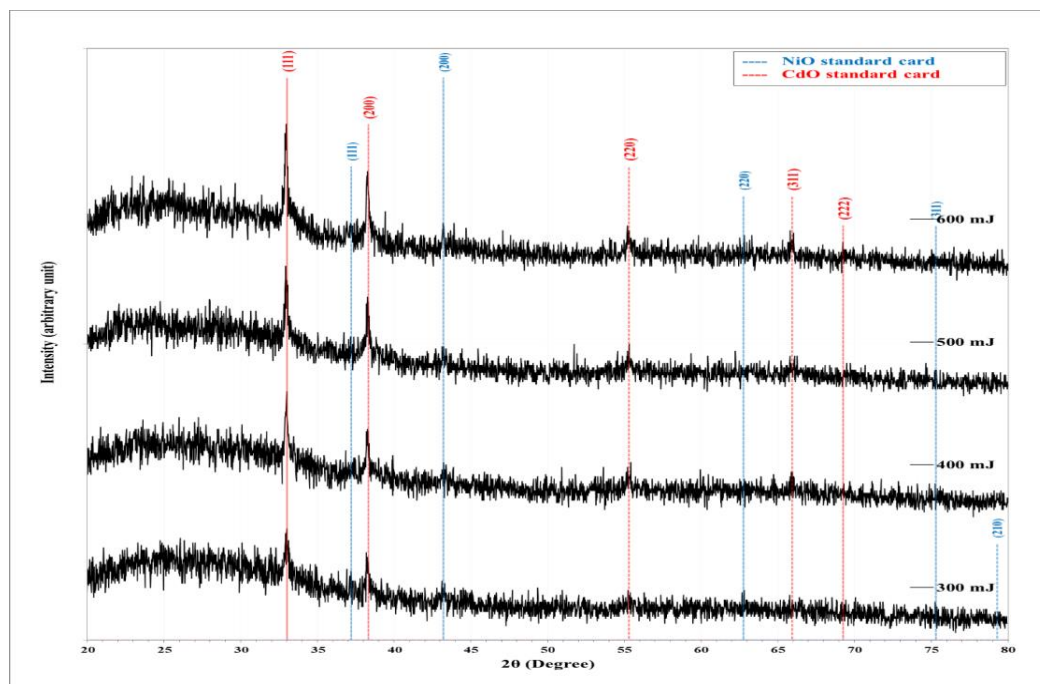


Figure 2-X-ray diffraction patterns of CdO: NiO composite thin films prepared by different laser energies.

Table 1-X-ray diffraction parameters for CdO: NiO thin films prepared by different laser energies.

Energy (mJ)	2θ (Deg.)	FWHM (Deg.)	d_{hkl} Exp.(Å)	G.S (nm)	d_{hkl} Std.(Å)	Phase	hkl
300	33.0280	0.5120	2.7099	16.2	2.7108	Cub. CdO	(111)
	38.2888	0.6106	2.3488	13.8	2.3477	Cub. CdO	(200)
	43.2561	0.5598	2.0899	15.3	2.0913	Cub. NiO	(200)
	55.3181	0.5597	1.6594	16.0	1.6600	Cub. CdO	(202)
400	32.9771	0.3563	2.7140	23.3	2.7108	Cub. CdO	(111)
	38.2697	0.4545	2.3500	18.5	2.3477	Cub. CdO	(200)
	43.2520	0.5088	2.0901	16.8	2.0913	Cub. NiO	(200)
	55.2672	0.5088	1.6608	17.6	1.6600	Cub. CdO	(202)
500	32.9262	0.4072	2.7181	20.3	2.7108	Cub. CdO	(111)
	38.2677	0.3053	2.3501	27.5	2.3477	Cub. CdO	(200)
	43.1952	0.4071	2.0927	21.0	2.0913	Cub. NiO	(200)
	55.2672	0.4579	1.6608	19.6	1.6600	Cub. CdO	(202)
	65.9033	0.4580	1.4162	20.7	1.4157	Cub. CdO	(311)
600	32.8753	0.3054	2.7222	27.1	2.7108	Cub. CdO	(111)
	37.2010	0.4589	2.4150	18.3	2.4148	Cub. NiO	(111)
	38.2667	0.2572	2.3501	32.7	2.3477	Cub. CdO	(200)
	43.1861	0.2545	2.0931	33.6	2.0913	Cub. NiO	(200)
	55.2163	0.4071	1.6622	22.0	1.6600	Cub. CdO	(202)
	65.9033	0.3562	1.4162	26.6	1.4157	Cub. CdO	(311)

The variation of lattice constant and lattice strain with laser energy are visualized in Figure 3. In both phases, it is clear that the constant lattice increases with increasing the laser energy while the lattice strain has the opposite behaviour. This is a consistent result, as increasing the laser power leads to an increase in the particle size as the small particles in the nanoscale have surface tension, which leads to a contraction of the lattice dimensions and correspondingly an increase in the lattice strain [18].

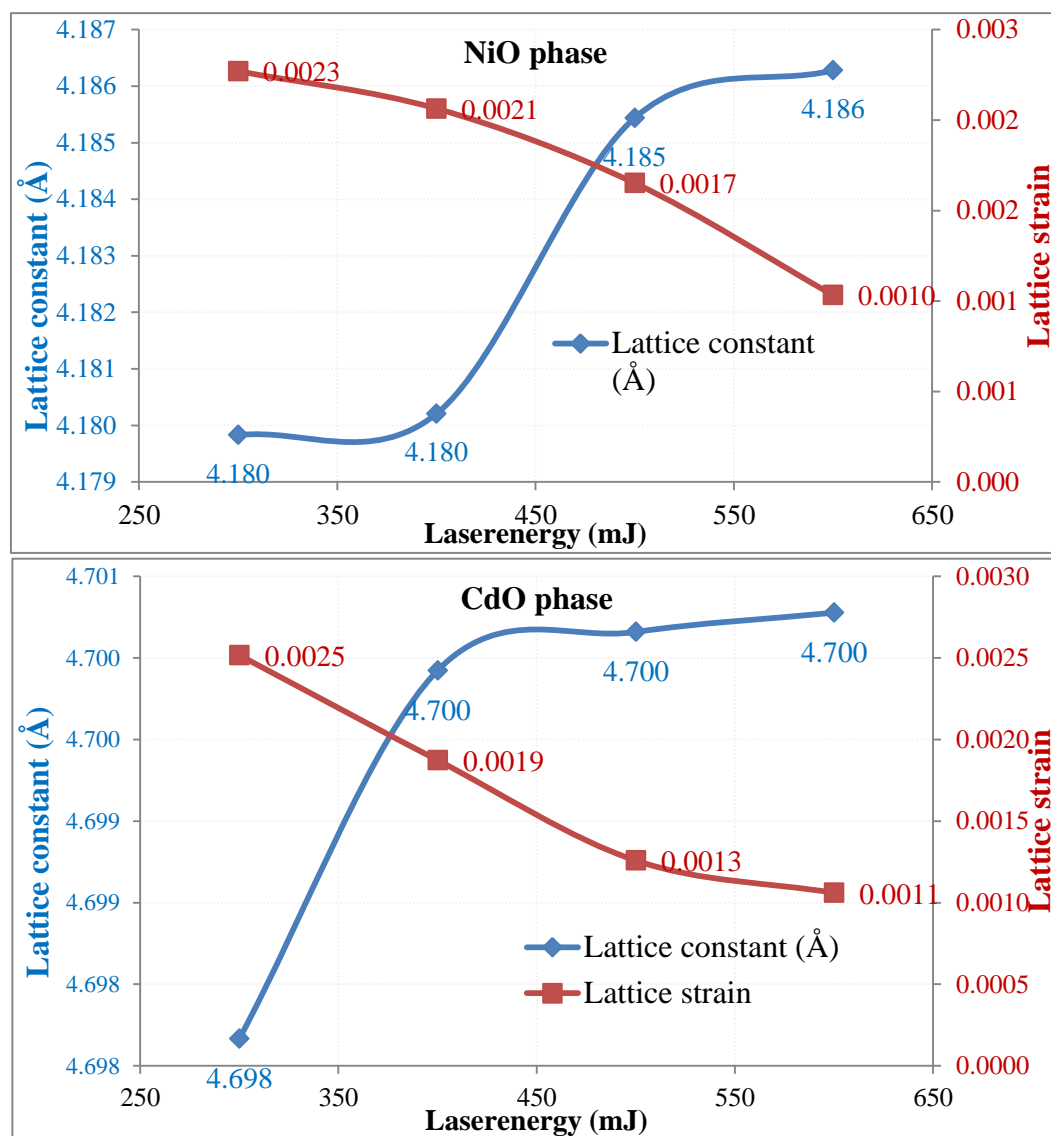


Figure 3-Variation of lattice constant and lattice strain for CdO and NiO crystals in CdO: NiO composite with laser energy.

Figure 4 shows the FESEM images, at two magnification powers, for CdO: NiO composite thin films prepared by a pulsed laser of different energies. The deposition appears to uniformly covering the entire surface without any cracks. The general structure consists of a well-connected structure consisting of small spherical particles ranging in size from 15 to 120 nm that are highly adhered to each other with few pores. The increase in the energy of the pulsed laser used in the deposition led to a gradual increase in the particles' size, but with irregular sizes and less connection between the particles, as gaps and cavities formed between the particles, forming a more porous structure. This high degree of porosity behaviour can be used in many fields of application, such as supercapacitor [19] or as an antibacterial layer etc. [20].

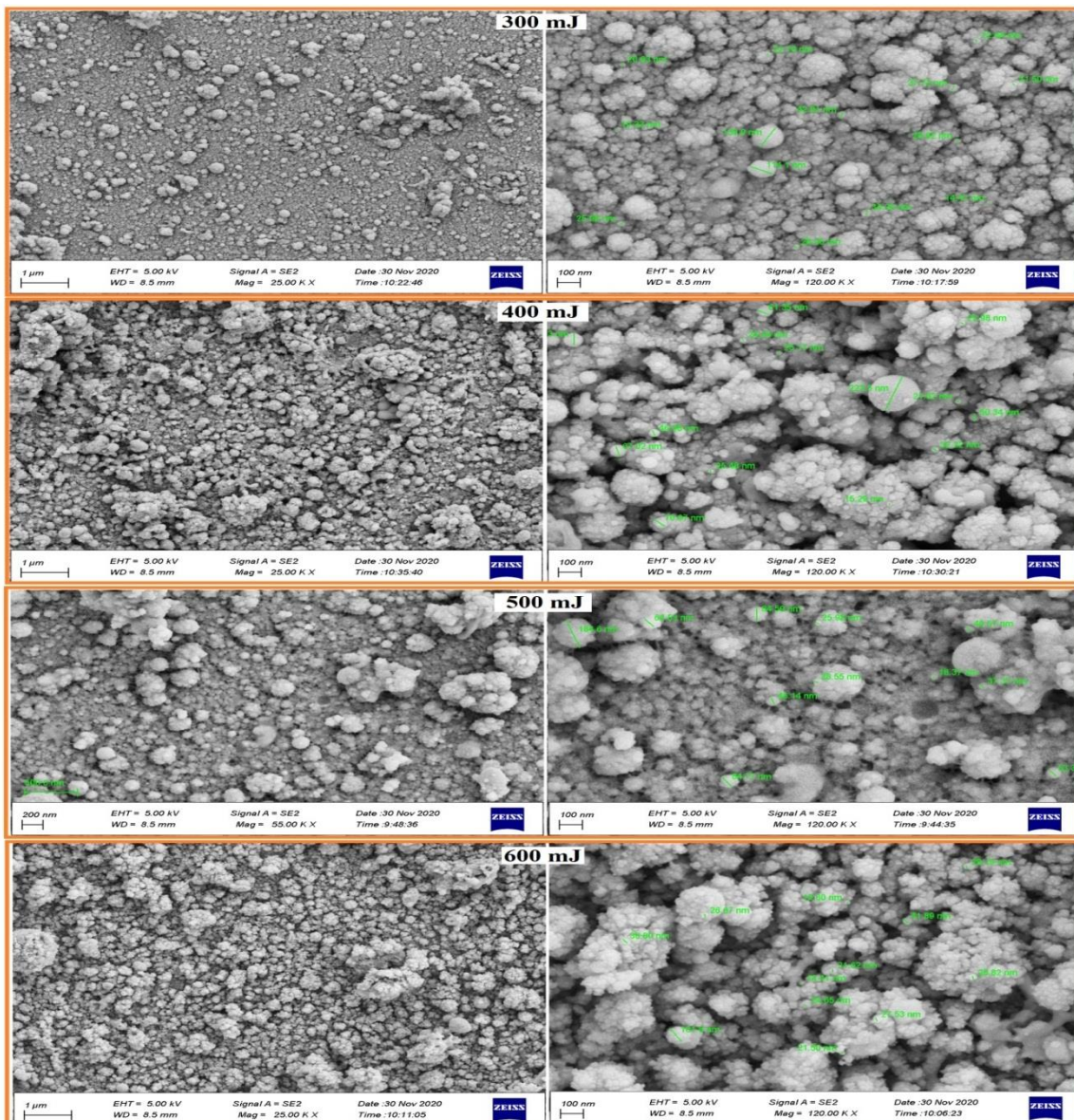


Figure 4-FESEM images at two magnification powers for CdO: NiO composite thin films prepared by different laser energies.

The EDX analysis for CdO: NiO composite thin films prepared by a pulsed laser of different energies were illustrated in Figure 5. The spectra of the samples consist of Cd, Ni, and O peaks. The additional peak at around 1.75 keV is for Si corresponding to the glass substrate. There were no strange peaks in the spectra of all samples indicating the purity of the samples. Ni/(Ni+Cd) percentage increased from 4% to 10% with increasing the laser energy from 300 mJ to 600 mJ due to the increase of the ablated NiO from targets. It is noticed from the figure that the percentage of nickel is very weak compared to cadmium due to the difference in the evaporation temperature of the two materials, and this agrees with the results of X-ray examinations.

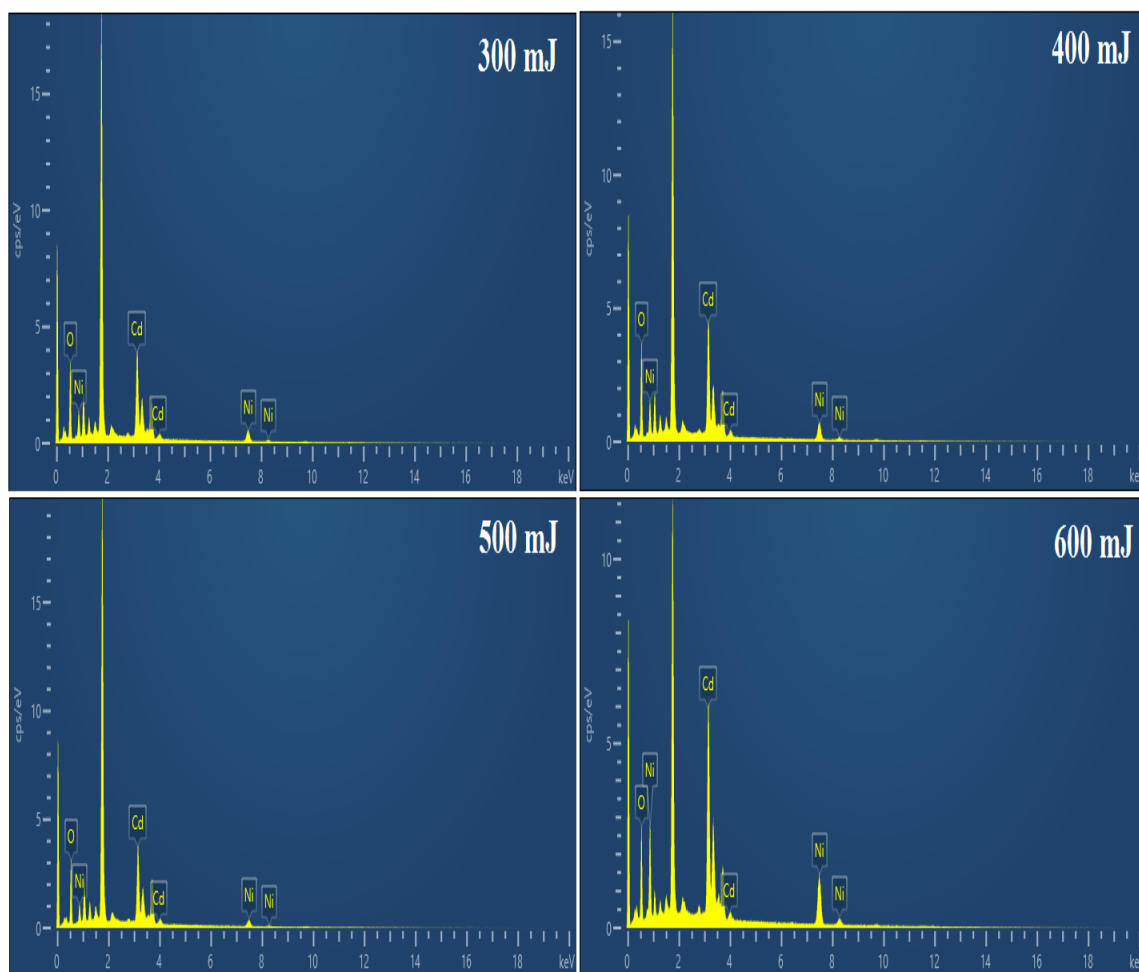


Figure 5-Elemental analysis for CdO: NiO composite thin films prepared by different laser energies.

Figure 6 shows the AFM images for CdO: NiO composite thin films prepared by pulsed laser at different energies and their size distribution. The sample prepared using the lowest energy was uniformly deposited on the entire surface, as shown by the 3D image and the particle size distribution. The increase of laser energy resulted in the increase of the average particle diameter and surface roughness. It can also be noticed that the particle distribution became irregular at high laser energy. Table 2 shows that the average diameter has increased from 62.29 nm to 110.58 nm and the surface roughness has increased from 6.5 nm to 20.3 nm, as the laser energy increased from 300 mJ to 600 mJ.

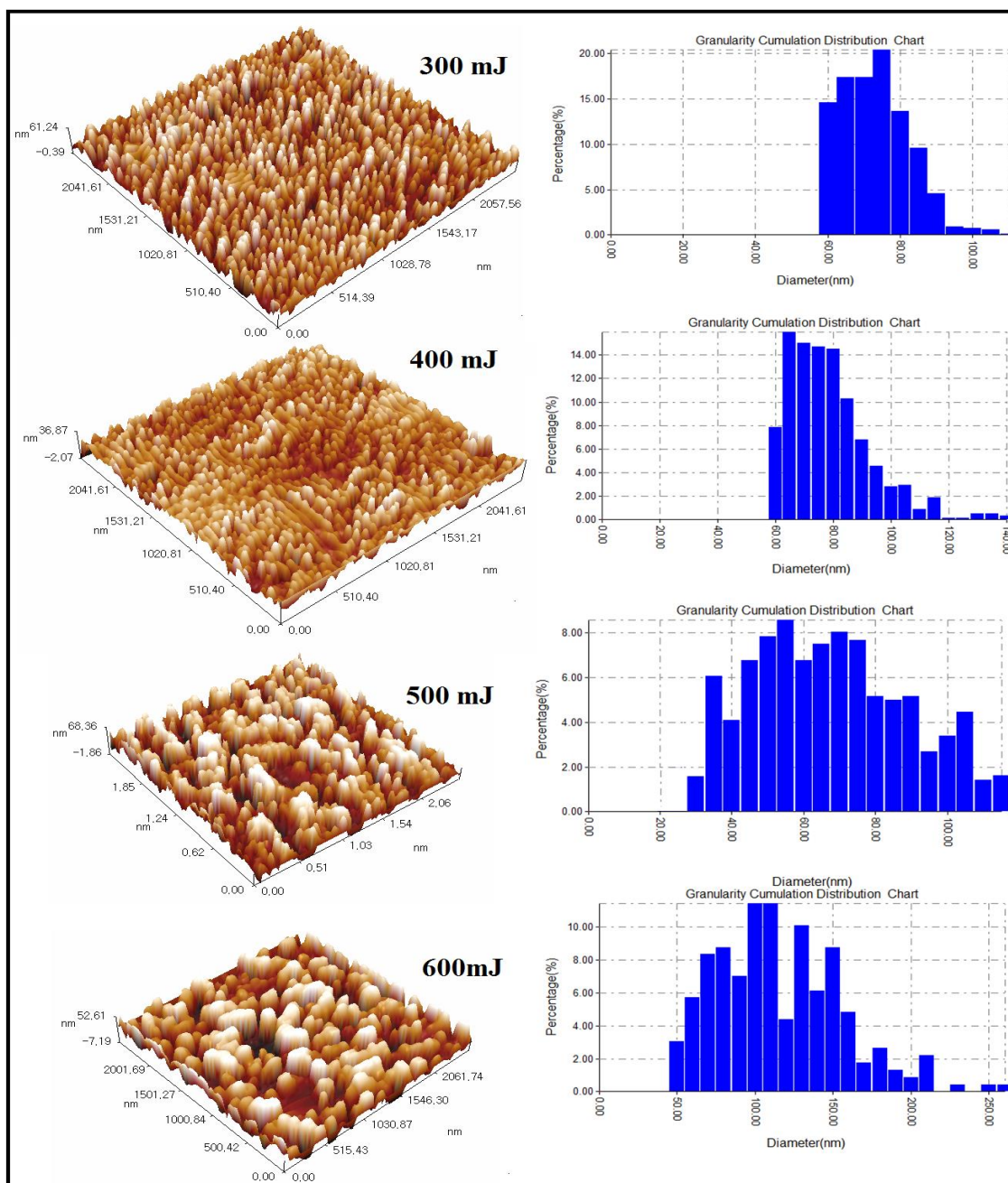


Figure 6-AFM images for CdO: NiO thin films and granulinity cumulating distribution prepared by different laser energies.

Table 2-AFM parameters for CdO: NiO thin films prepared by different laser energies.

E (mJ)	Average Diameter (nm)	RMS roughness (nm)	Roughness Ave. (nm)
300	62.29	5.25	6.5
400	70.54	12.2	14.4
500	76.36	15	17.3
600	110.58	17.6	20.3

Figure 7 shows the absorbance curves for the CdO: NiO thin film samples prepared by different laser energies. It appears that the absorbance gradually decreased with wavelength indicating low crystallinity for all the prepared samples. It was also observed that the absorbance increased with increasing laser energy due to the increase of the ablated material from the target, causing the increase of film thickness.

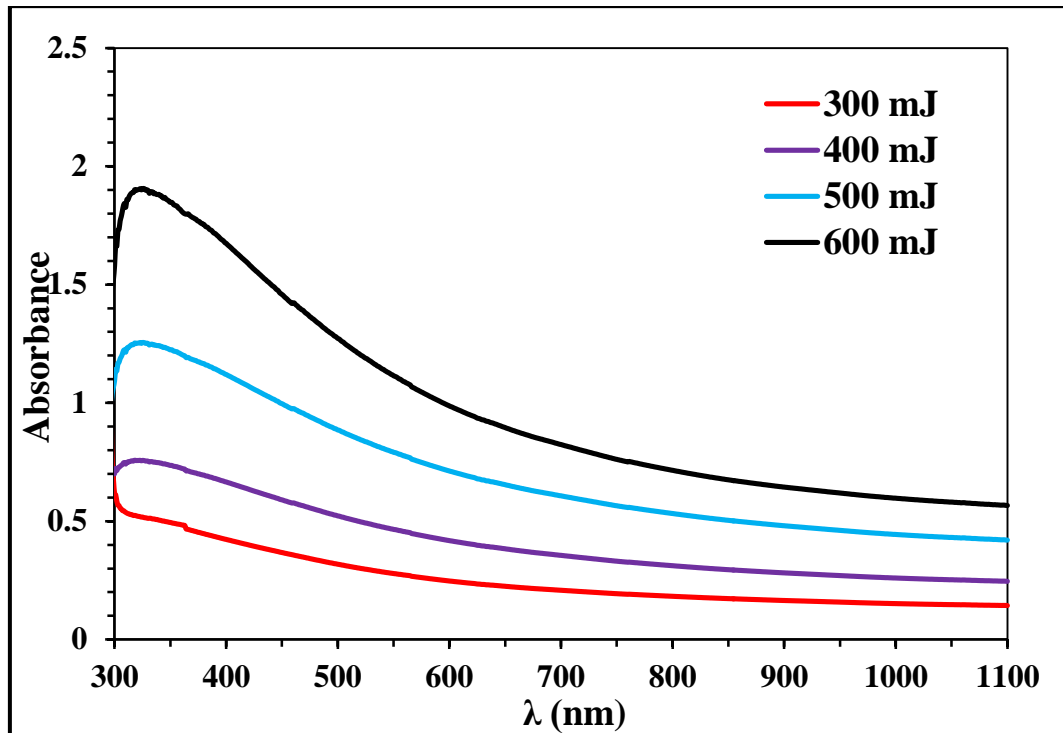


Figure 7- UV-visible absorbance spectra for CdO: NiO thin films prepared by different laser energies.

The optical energy gap values (E_g^{opt}) for CdO: NiO thin films prepared by pulsed laser were determined using the Tauc equation, as shown in Figure 8. The optical band gap varies from 2.4 to 2.25 eV with increasing laser energy from 300 to 600 mJ. This result is due to the increase of particle size as shown by FESEM measurements, thus reducing the quantum confinement effect for nanoparticles [21]. Naser et al. found that the energy gap values of the mixture are close to the energy gap values for the cadmium oxide thin films [22], and this is consistent with the results of the X-ray diffraction and EDX assays.

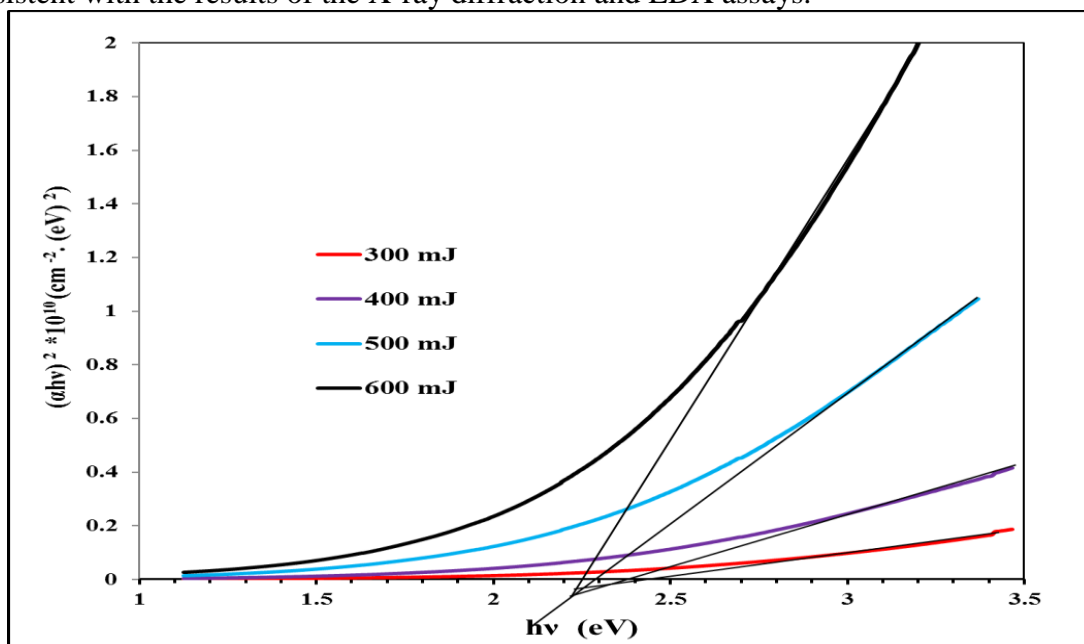


Figure 8- Calculation of energy gap for CdO: NiO thin films prepared by different laser energies.

The results obtained from the Hall measurements showed that the CdO: NiO thin films were n-type due to oxygen vacancies. These results agree with those of Calnan [23]. The charge carrier (n_H) and mobility (μ_H) were calculated using the Hall coefficient for each sample. The variation of n_H and μ_H with laser energy are illustrated in Figure 9. It was found that the charge carrier concentration decreased, due to the reduction of oxygen vacancies, as shown by the EDX analysis. At the same time, mobility μ_H increased with increasing laser energy. Such behaviour is expected, as the particle size increases with increasing laser energy by removing the grain boundaries, which leads to increased charge carrier mobility.

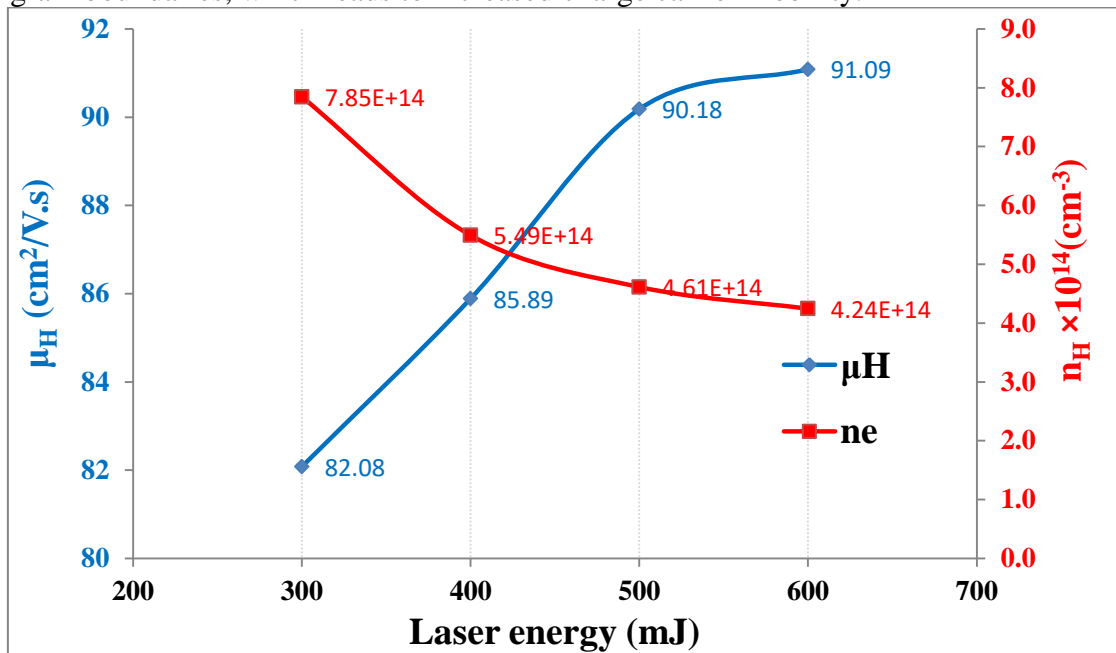


Figure 9-Variation of n_H and μ_H coefficients for CdO, NiO and CdO: NiO with laser energy.

The I-V characteristic curves for CdO: Ni/P-Si heterojunction prepared by different laser energies in the dark and under illumination using power densities of $100 \text{ mW}/\text{cm}^2$ with applied forward and reverse bias are shown Figure 10. In general, the forward current is higher than the reverse current. The depletion region width decreases with the increase of the applied forward voltage, which causes a high current. Simultaneously, the reversed process occurs for the reverse bias, indicating the junction formed between the substrate and the deposited material. The samples under illumination showed photovoltaic effect (there is a cross-area in the fourth quarter). The short circuit current (I_{sc}) and open-circuit voltages (V_{oc}) were calculated from the cut-off curve with the y-axis and x-axis. Also, the largest power was calculated from the most extensive area that can be drawn inside the cross area. The filling factor (FF) and solar cell efficiency (η) were calculated from these quantities.

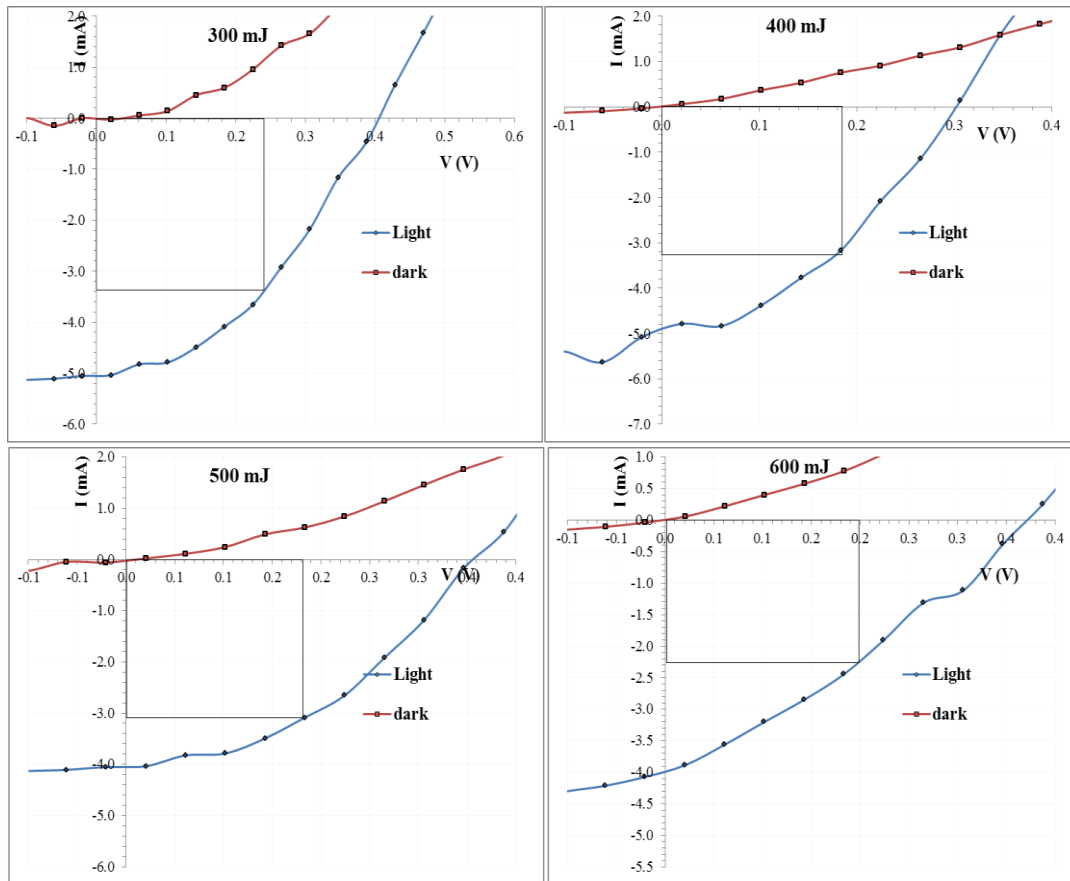


Figure 10- I-V characteristic curves for CdO: NiO/p-type Si heterojunction prepared by different laser energies.

Figure 11 shows the relation between $\ln(I)$ and the applied forward bias voltage in the dark for CdO: NiO/PSi heterojunction. These curves were used to calculate the ideality factor using the relation [24].

$$I = I_s \exp\left(\frac{qV}{\beta K_B T}\right)$$

Where: I_s is the saturation current, q is the electron charge, V is the applied voltage, K_B Boltzmann constant, T absolute temperature, and β is the ideal factor. The ideality is calculated from the slope of the linear part of the curves from $V=0$ to $0.3V$.

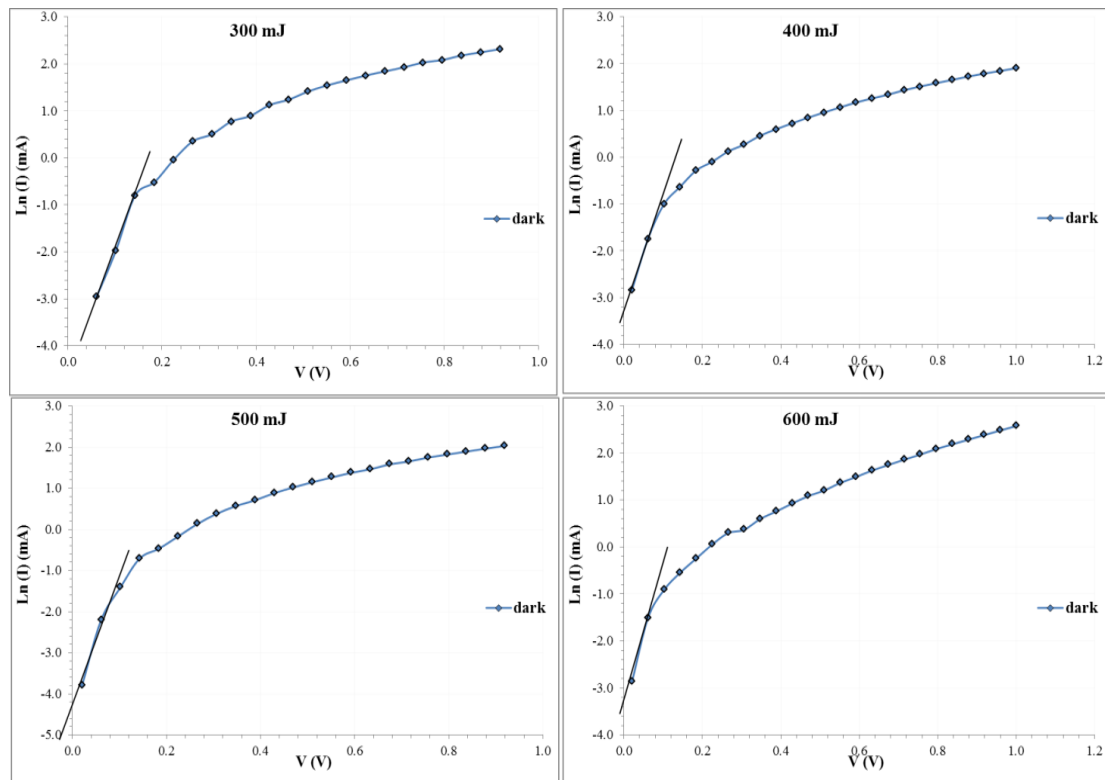


Figure 11- ln(I) vs.V for CdO:NiO/p-type Si heterojunction prepared by different laser energies.

Table 3 shows the solar cell parameters for CdO: NiO/p-type Si heterojunctions prepared by different laser energies. It seems that the optimum solar efficiency of 0.14% for CdO/PSi and 0.816% for CdO: NiO/PSi was for the samples prepared with the lowest laser energy. This is due to their higher transparency (as shown by the UV visible absorbance) which allows the photons to reach the junction and also because of high carrier concentration which contributes in electrical current. The table shows that the ideal factor values are high and this is due to the formation of cell layers of different materials, which leads to a high leakage current thus a high ideal factor.

Table 3- photovoltaic parameters for the heterojunctions prepared by different laser energies.

E (mJ)	I _{sc} (mA)	V _{oc} (V)	I _m (mA)	V _m (v)	F.F	η%	β
300	5.000	0.400	3.400	0.240	0.408	0.816	3.208
400	5.000	0.300	3.300	0.190	0.418	0.627	3.422
500	4.000	0.360	3.200	0.180	0.400	0.576	2.624
600	4.000	0.370	2.300	0.200	0.311	0.460	3.214

4. Conclusions

Study the characteristics of CdO: NiO composite thin films prepared by pulsed laser deposition showed that it is possible to control thin films properties by changing the laser energy used in their preparation. The final substance has new properties for a combination of both materials. However, it should be noted that both XRD and EDX showed the predominance of cadmium oxide content over nickel oxide in the prepared films. The X-ray diffraction for the CdO: NiO composite thin films showed mixed phases of the significant CdO phase with the minor phase of NiO structure. Increasing the laser energy resulted in increase of crystallinity and lattice constants, while the lattice strain had the opposite

behaviour. The FESEM images for the CdO: NiO thin films to cover the entire surface without any cracks well-connected structure uniformly consists of small spherical particles, their size from 15 to 120 nm. An increase in laser energy caused irregular increase in the particles size.

The EDX analysis proved the purity of the samples, that they contained the characteristic elements and increases their content, and increases oxidization in samples with laser energy, especially at the 600 mJ. The AFM for the created porous silicon seemed to contain many pores of different sizes. The average pore diameter was 34.40 nm. The AFM for the deposited thin film at the lowest laser energy was uniformly deposited on the surface. The increase of laser energy caused the increase of the average particle diameter and surface roughness. The absorbance for all deposited thin film samples increased with increasing laser energy with red shifting of the absorbance edge. In contrast, the optical band gap decreases with increasing laser energy due to the particle size increase. Hall effect measurements showed that the CdO and CdO: NiO thin films were n-type, while the NiO samples were p-type. The charge carrier concentration decreased due to reduced oxygen vacancies, while the mobility μ_H increases. The I-V characteristics for CdO: NiO/porous-PSi heterojunctions prepared by different laser energies show photovoltaic properties. The optimum efficiency was for samples prepared using the lowest laser energy due to the higher transparency and high carrier concentration contributing to electrical current.

Although the efficiency of the obtained heterojunctions is low, the cost of preparing them is very low. Besides, they can be used as a photodetector. Also, devices made up from metal oxides have high chemical stability.

References

- [1] T. K. S.Wong, S. Zhuk, S. Masudy-Panah, and G. K. Dalapati, "Current Status and Future Prospects of Copper Oxide Heterojunction Solar Cells," *Materials (Basel)*, vol. 9, no. 4, pp. 271, 2016.
- [2] A. M. Mostafa, S. A. Yousef, W. H. Eisa, M. A. Ewaida, and E. A. Al-Ashkar, "Synthesis of cadmium oxide nanoparticles by pulsed laser ablation in liquid environment," *Optik (Stuttg.)*, vol. 144, pp. 679–684, 2017.
- [3] A. Alemi, S. W. Joo, S. Khademinia, M. Dolatyari, and A. Bakhtiari, "Sol – gel synthesis , characterization, and optical properties of Gd 3+ -doped CdO sub-micron materials," *Int. Nano Lett.*, vol. 3, no. 3, pp. 2–7, 2013.
- [4] J. K. Rajput, and L. P. Purohit, "Comparative Study of Synthesis of CdO-ZnO Nanocomposite Thin Films by Different Methods: A Review," *Nanosci. Technol. Open Access*, vol. 3, no. 2, pp. 1–5, 2016.
- [5] G. Bangaru, P. Matheswaran, and R. Sathyamoorthy, "Influence of Annealing on Physical Properties of CdO Thin Films Prepared by SILAR Method," *J. Mater. Sci. Technol.*, vol. 29, no. 1, pp. 17–21, 2013.
- [6] R. Chandiramouli and B. G. Jeyaprakash, "Review of CdO thin films," *Solid State Sci.*, vol. 16, pp. 102–110, 2013.
- [7] M. Zaien, N. M. Ahmed, and Z. Hassan, "Fabrication and characterization of an n-CdO/p-Si solar cell by thermal evaporation in a vacuum," *Int. J. Electrochem. Sci.*, vol. 8, no. 5, pp. 6988–6996, 2013.
- [8] H.H.Murbat | N. KH. Abdalameer| A. Kh.Brrd| F.abdulameer, "Effects of Non-Thermal Argon Plasma Produced at Atmospheric Pressure on the Optical Properties of CdO Thin Films," *Baghdad Sci. J.*, vol. 15, no. 2, pp. 221–226, 2018.
- [9] K. Usharani and A. R. Balu, "Structural, optical, and electrical properties of Zn-doped CdO thin films fabricated by a simplified spray pyrolysis technique," *Acta Metall. Sin. (English Lett)*, vol. 28, no. 1, pp. 64–71, 2015.
- [10] K. Siraj, M. Khaleeq-Ur-Rahman, S. I. Hussain, M. S. Rafique, and S. Anjum, "Effect of deposition temperature on structural, surface, optical and magnetic properties of pulsed laser deposited Al-doped CdO thin films," *J. Alloys Compd.*, vol. 509, no. 24, pp. 6756–6762, 2011.

- [11] M. M. Arafat, B. Dinan, S. A. Akbar, and A. S. M. A. Haseeb, "Gas Sensors Based on One Dimensional Nanostructured Metal-Oxides: A Review," *Sensors(Basel)*, vol. 12, NO. 6, pp. 7207–7258, 2012.
- [12] R. Koole, E. Groeneveld, and D. Vanmaekelbergh, *Size Effects on Semiconductor Nanoparticles*.
- [13] T. Ahmad, S. Khatoon, K. Coolahan, and S. E. Lofland, "Structural characterization, optical and magnetic properties of Ni-doped CdO dilute magnetic semiconductor nanoparticles," *J. Mater. Res.*, vol. 28, no. 9, pp. 1245–1253, 2013.
- [14] A. A. Dakhel, "Study of high mobility carriers in Ni-doped CdO films," *Bull. Mater. Sci.*, vol. 36, no. 5, pp. 819–825, 2013.
- [15] E. F. Abo Zeid, I. A. Ibrahim, A. M. Ali, and W. A. A. Mohamedd, "The effect of CdO content on the crystal structure, surface morphology, optical properties and photocatalytic efficiency of p-NiO/n-CdO nanocomposite," *Results Phys.*, vol. 12, pp. 562–570, 2019.
- [16] M. Nazarian-Samani and A. R. Kamali, "Characteristics of thermal transitions during annealing of a nanocrystalline Ni₃Al-based alloy," *J. Alloys Compd.*, vol. 486, no. 1–2, pp. 315–318, 2009.
- [17] P. T. Ranjani, P. D. Raj, B. L. Shree, S. S. Priya, and P. Karthick, "Studies on Magnetron Sputtered V₂O₅ Thin Films Deposited over ZnO Buffer Layer," *Mater. Today: Procs.*, vol. 3, no. 6, pp. 1477–1486, 2016.
- [18] Z. Huang, P. Thomson, and S. Di, "Lattice contractions of a nanoparticle due to the surface tension: A model of elasticity," *J. Phys. Chem. Solids*, vol. 68, no. 4, pp. 530–535, 2007.
- [19] M. Liu, J. Chang, J. Sun, and L. Gao, "Synthesis of porous NiO using NaBH₄ dissolved in ethylene glycol as precipitant for high-performance supercapacitor," *Electrochim. Acta*, vol. 107, pp. 9–15, 2013.
- [20] N. Behera, M. Arakha, M. Priyadarshinee, B. S. Pattanayak, S. Soren, S. Jha, and B. C. Mallick, "Oxidative stress generated at nickel oxide nanoparticle interface results in bacterial membrane damage leading to cell death," *RSC Adv.*, vol. 9, no. 43, pp. 24888–24894, 2019.
- [21] S. Sapra, D. D. Sarma, S. Sanvito, and N. A. Hill, "Influence of Quantum Confinement on the Electronic and Magnetic Properties of (Ga,Mn)As Diluted Magnetic Semiconductor," *Nano Lett.*, vol. 2, no. 6, pp. 605–608, 2002.
- [22] G. Y. Naser, W. N. Raja, A. S. Faris, Z. J. Rahem, M. A. Saleh, and A. H. Ahmed, "Some optical properties of CdO thin films," *Energy Procedia*, vol. 36, pp. 42–49, 2013.
- [23] S. Calnan, "Applications of Oxide Coatings in Photovoltaic Devices," *Coatings*, vol. 4, no. 1, pp. 162–202, 2014.
- [24] SethuRaman, N. Senthilkumar, J. Chandrasekaran, R. Priya, P. Baraneedharan, Murthy Chavali
- [25] M. S. Raman, N. Senthil, J. Chandrasekaran, R. Priya, P. Baraneedharan, and M. Chavali, "Thermal annealing effects on structural, optical and electrical properties of V₂O₅ nanorods for photodiode application," *Optik (Stuttg.)*, vol. 157, pp. 410–420, 2018.